v. 5, n. 4, 2025

International Journal of Biological and Natural Sciences

Acceptance date: 22/07/2025

OTOLITH MICROSTRUCTURE REVEALS FIRST SEXUAL MATURITY AS THE MAIN EVENT IN THE FORMATION OF THE FIRST YEAR RING IN ANCHOVY *ENGRAULIS ENCRASICOLUS* IN NORTH ALBORAN SEA

Javier Rey
Instituto Español de Oceanografía-CSIC. Centro Oceanográfico de Málaga. Explanada de San Andrés s/n. Muelle 9. 29002 Málaga (Spain)
Instituto de Ingeniería Oceánica. Escuela Técnica Superior de Ingeniería de Telecomunicación. Universidad de Málaga. Bulevar Louis Pasteur nº35. 29010 Málaga (Spain)

María del Carmen Clemente
Instituto de Ingeniería Oceánica. Escuela Técnica Superior de Ingeniería de Telecomunicación. Universidad de Málaga. Bulevar Louis Pasteur nº35. 29010 Málaga (Spain)

Miriam Domínguez
Instituto Español de Oceanografía-CSIC. Centro Oceanográfico de Málaga. Explanada de San Andrés s/n. Muelle 9. 29002 Málaga (Spain)

Ivone Czerwinski
Instituto Español de Oceanografía-CSIC. Centro Oceanográfico de Cádiz. Puerto Pesquero, Muelle de Levante, s/n. 11006 Cádiz (Spain)

Pedro Torres
Instituto Español de Oceanografía-CSIC. Centro Oceanográfico de Málaga. Explanada de San Andrés s/n. Muelle 9. 29002 Málaga (Spain)

Abstract: Several studies have recently been published on measuring the age and growth of anchovy based on otolith microstructure, although the methodologies used were not analogous or easily reproducible. The three--dimensional complexity and heterogeneity of otoliths make establishing common interpretation criteria difficult. In the search for a simple and reproducible reading process, this study contrasts a different alternative, combining analysis of otolith frontal sections at two magnifications (×200 and ×400). The results of this study point to the frontal plane of the otolith at ×200 magnification as an improved method to determine the age of the anchovy through the microstructure, both in terms of reproducibility and precision. In addition, the readings of the daily growth increments (DGI) of the otolith sections indicated that in the first year of life the Alboran anchovy reaches 16.52 cm and that the seasonal ring defined by the otolith macrostructure of the first year corresponds to a winter ring that coincides with the first sexual maturation event. The DGI count has also been used to establish the most likely birth dates in July, coinciding with the anchovy spawning season in the area.
Keywords: Age determination; daily growth; small pelagics; sectioned otoliths; microstructure; validation

INTRODUCTION

Knowing and quantifying parameters such as growth, mortality and recruitment is of paramount importance in fisheries, enabling assessment of populations subject to fisheries exploitation and, therefore, facilitating advice on the state of stocks (Hilborn and Walters, 1992). These parameters are strongly linked to fish age. Consequently, the recognition and quantification of certain time marks on calcified structures of the exploited species, particularly in fish otoliths, is practical for managing marine resources stocks (Panfili

et al., 2002). Changes of an endogenous and exogenous nature leave marks in the calcified structures whose differentiation can produce uncertainties in age estimation (Dortel et al., 2013). Sclerochronology can still provide much information on the interaction between marine life and its environment, including the effects of a changing climate (Hunter et al., 2018), thus allowing for a deep understanding of fish growth.

Age data are globally used in fisheries to assess and manage marine exploited resources, to facilitate their sustainable exploitation (Campana and Thorrold, 2001). Extensive economic and human resources have been committed to acquiring age data from diverse fish species, yet ageing criteria are oftentimes not validated (Beamish and Farlane, 1983; Campana, 2001), despite scientific efforts to ameliorate ageing criteria on behalf the international scientific entities (e.g., ICES Working Groups on Biology and Growth). The understanding of otolith accretion in the form of daily rings (Panfili et al., 2002; Campana, 2005; Rey et al., 2016) has led to the development of new tools focused on otolith microstructure analyses through the mediation of growth experts and engineering expertise (Nava et al., 2018).

Age data of European anchovy (*Engraulis encrasicolus*, L. 1758) sampled daily will be used to assess growth through a novel approach that interprets daily age data from the sagittal and frontal sections of otoliths, similar to the method applied to European hake (Piñeiro et al., 2008). The target species is a small pelagic fish from the Mediterranean Sea, although its distribution encompasses an extensive area, from Norway to Angola, as well as the Mediterranean, Black Sea and Sea of Azov (Whitehead et al., 1988). In the Mediterranean, it is one of the most exploited species due to its commercial importance, and as such is considered overexploited in many of its regions (Palomera et al., 2007, Torres et al, 2022). The species is characterised by a short lifespan, seasonal migrations, high growth rates, which vary according to seasonality and distributional area, early maturity and a long spawning period (Uriarte et al., 1996; Palomera et al., 2007; Giráldez, 2012). The maximal standard length registered for anchovy is about 20 cm, the common length is about 13.5 cm (Whitehead et al., 1988) and the maximum reported age is five years (ICES, 2016). In the Alboran Sea, the maximum reported size and age were 18.5 cm and three years (3+) between 1990 and 2019 (Torres et al., 2022).

In recent years, numerous workshops have been organised in the ICES area focused on the validation of growth rings and the standardisation process among labs and areas within European waters (ICES 2013, 2016, 2019 and 2023), particularly in short-lived pelagic species. Recommendations include furthering methods that enable more precise and accurate readings between experts (ICES, 2019). The main reported difficulties in estimating ages of anchovy are: i) differentiation between annual (winter) and false rings; ii) recognition of weakly marked winter rings; iii) insufficient criteria on annual growth patterns and iv) recognition of the opaque/hyaline nature of the otolith edge (ICES, 2016).

Otoliths are calcareous structures located in the saccule of the inner ear, specifically in the vestibular system of teleost fish (Panfili et al., 2002). These structures grow three-dimensionally throughout the life of the fish and are the only ones that register irregularities (marks) that can be related to different time scales: seasonal (macrostructure) and daily (microstructure). The external (environmental) and internal (physiological) events that influence individual growth leave marks (layers) on otoliths that can be interpreted (placed in lifetime) with the appropriate tools and knowledge. Consequently, otoliths (whole and in sections) have been broadly used to

age fish, mainly by means of seasonal marks. Particularly, two-dimensional otolith sections facilitate mark analysis and may include the centre or nucleus (birth date) and edge (death date) of the otolith, covering the entire lifespan. For otolith sectioning, three orthogonal planes are possible—sagittal, transversal and frontal (Figure 1a)—and are therefore used for sclerochronological studies (Panfili et al., 2002; Wright et al., 2002). Sagittal and transverse sections have been most used to age both pelagic and demersal fish. Each section shows growth marks (age information) along different otolith axes. To compare growth marks, increment counts and measurements of different otoliths sections are analysed along the same axis.

The wider winter seasonal growth rings are normally used to assign ages. Those of lesser relevance are considered checks or false rings. In anchovy, both types are typified by experts (Villamor, 2019). The coherent interpretation of the different checks or rings is usually difficult and subjective, which is why agreement between experts is needed to set up common criteria for selecting the appropriate growth rings. Furthermore, agreements must be supported by validation studies, which offer alternative results that sustain these criteria. In anchovy, although an ageing criterion is established and supported by validation studies (Cermeño et al., 2008; Uriarte et al., 2016; Basilone et al., 2020), there is still considerable uncertainty in age estimation by otolith macrostructure readings (Basilone et al., 2020). These disparities between researchers may also arise because anchovy validations were undertaken on fishes from two different areas: the Atlantic and the Sicilian Channel region. Therefore, a further validation study on anchovy from the Alboran Sea is fully justified.

The goal of this study is twofold: *i)* to contrast a different otolith section (frontal) at two magnifications (×400 and ×200), to set up an improved alternative to the routine ageing of anchovy and *ii)* to validate the first annulus (year) assigned by macroscopic examinations by means of the daily ring count.

MATERIAL AND METHODS

SAMPLING AND SAMPLES PREPARATION

Samples were collected from research pelagic trawl surveys and onshore samplings, from January to December 2014, in the North Alboran Sea, following the principles of national and international animal ethics. Total length (TL, in mm) was recorded from sampled *E. encrasicolus* individuals, and sagitta otoliths were removed onboard from random selected individuals (70–170 mm) and stored in vials. Two independent collections were set since processes are different and not compatible: 1) A sample of 793 anchovy otoliths were selected for ageing by means of annual rings (macrostructure) and 2) independently, 106 otoliths (53 pairs) were selected for microstructure analysis.

The 793 pairs of otolith, covering the whole size range were mounted on black plates and fixed with "Eukitt" resin (Table 1). Separately, the collection of 53 pairs of otoliths were embedded in polyester resin (Buehler Epoxi 20-3440-022), encompassing the whole size range (Table 1). Vials were filled with up to 1 cm of resin bed. Once the resin had attained the appropriate solidity (approximately 2–3 hours later), the otoliths were placed sulcus side up and fixed with instant glue (Loctite®). The otoliths were later covered with an additional layer of resin of the same thickness and left for 24 hours to ensure total crystallisation. Samples were then polished with a Metaserv 250 Grinder-Polisher equipment (sandpaper used: Buehler silicon carbide grinding paper, 120p and 1200p).

Left otoliths were polished on the sagittal plane (Figure 1a, b) until the sulcus was eliminated and the nucleus and daily growth increments (DGI) were visible. Right otoliths were polished similarly until the centre was reached on the frontal plane (Figure 1a, b). In both cases, polished faces were fixed on a methacrylate slide. Once completely glued (24 hours), the otoliths were polished from the other side to obtain a final sample with an approximate width of 50–120 μ that would subsequently facilitate the reading procedure. The width of the sagittal (SS) and frontal sections (FS) was controlled throughout the laboratory polishing process with a precision micrometre, and the quality of the polished section was continually examined under a microscope.

READING PROCEDURE

Anchovies were aged by means of macrostructure (whole otoliths) following the standards established by the International Council for Exploration of the Sea (ICES) (ICES, 2023), 1 July being taken as the birth date. Anchovy growth during the first year was estimated by measuring the first annual ring radius (R1) on digitised photographs of the otoliths (Figure 2a) with a stereomicroscope (Leica EZ4 HD, x20) and Image J software (Schneider et al, 2012). R1 was defined as the distance (in mm) between the core and the inner edge of the first hyaline ring, and was measured across the posterior axis, the same axis used to estimate the age of fishes by means of their otolith microstructures. If the individual was captured after 1 July, the hyaline ring visible on the otolith edge was not considered to be an R1, as recommended by ICES (ICES, 2009). Mean distance measurements of the first visible annulus were then analysed, taking into account the date of fish capture (Ventero et al., 2017). Because the length of the anchovy otolith R1 can be considered as an indicator of first-year growth (Hernández et al., 2013), distances to the first hyaline annulus (that should correspond to the first annual ring) were measured and their mean calculated for subsequent comparison with our microstructural measurements. The first hyaline ring may be a check or false ring and in ICES 2016 and 2023 reports is clearly stated that annual rings are preferably assigned if the radius is higher than 0.8 mm.

Polished otoliths were analysed under a microscope (Leica CTR6 LED) with transmitted white light, coupled with a digital camera (Leica DFC 7000 T) connected to a computer. FS were observed ('read') at ×200 and ×400 magnifications throughout the posterior growth axis, from the centre to the edge (Figure 1b and Figure 2 b). The central zone of the SS (CZ_S) around the nucleus was also observed at x1000 magnification for a more precise study of the larval life phase (Figure 1b, Figure 2c).

Image acquisition and storage of overlapping images (with 10–20% overlapping area) gave a final single panoramic view of the full otolith from the combined partial, overlapped images. For DGI counting and width--measuring, the novel image software OTOLab was used (Nava et al., 2018). This free software platform is specifically designed for application in otolith studies. The OTOLab software can be freely downloaded from www.ieo.es/es/otolab_2019.

The highest magnification (×1000) was used for reading the CZ_S of SS in immersion oil, where DGI are usually narrower and more difficult to interpret. The outer part of the otolith was read at ×200 and ×400, in and FS.

Since most studies of anchovy otoliths recommend the posterior axis (postrostrum axis) for examining microstructure (Cermeño et al., 2008; ICES, 2013), we chose this reference axis for DGI analysis (Figure 1). All increments were measured and counted, starting at hatch increment or first feeding check (FFC)

(Aldanondo et al., 2008, 2010). Distances between increments were always measured along the same axis from the core to the edge along the postrostrum side. As DGI deposition has been validated for European anchovy larvae (Aldanondo et al., 2008) and juveniles (Cermeño et al., 2003), the increment number was considered as a proxy of age in days.

However, the central zone of frontal sections was frequently dark or shadowed, or the DGI were not discernible (Figure 2b). Therefore, we performed a linear relationship between the number of DGI that were possible to read in the CZ_S and the read radius of CZ_S (Piñeiro et al., 2008). This linear relationship was applied to estimate the number of increments within the central zones when this area was not legible (Rey et al., 2016). Finally, these estimated ages were added to the increment counts observed throughout the discernible parts of the otoliths, to estimate the total age of individuals.

With OTOLab, partial images were merged into panoramic views. The merged images enabled us to draw a polyline from the nucleus (birth) to the otolith edge of the posterior growth axis, corresponding to the date of capture, and thus the death of the specimen (Figure 2b). OTOLab allows the reader to point out increments along the polyline (Figure 2). Once DGI are measured and counted throughout the whole reading axis, data are stored in OTOLab and exported to a spreadsheet for otolith microstructure analysis. In cases where the reading procedure was not possible around the nucleus, the readings performed in the SS at x1000 were added to the age estimated with OTOLab.

ASSESSING ANCHOVY GROWTH MODELS

The growth data from both reading methods or factors (FSx200 and FSx400) were analyzed using the von Bertalanffy Growth Model (VBGM). Data sets included measurements of age (in fractions of a year) and size (TL, cm). Growth models were fitted separately for each group using the `nls` function in R. The formula for the VBGM used was:

$$Size = L_\infty * (1 - \exp(-K * (age - t_0))),$$

where L_∞ is the asymptotic length, K is the growth rate, and t_0 is the hypothetical age at which the size is zero. Initial parameter values were set as $L_\infty = \max(size)$, $K = 2$, and $t_0 = 0$. To compare the growth models between FSx200 and FSx400, the `growthlrt` function from the fishmethods package (Nelson, 2023) was used. Following Kimura (1980), for each general model-sub model comparison, likelihood ratios are calculated by using the residual sum-of-squares and are tested against chi-square statistics with the appropriate degrees of freedom to assess the significance of differences in growth parameters (L_∞, K, t_0) between the two groups. Four hypotheses were tested: 1) $L_{\infty 1} = L_{\infty 2}$, 2) $K_1 = K_2$, 3) $t_{01} = t_{02}$ and 4) $L_{\infty 1} = L_{\infty 2}$, $K_1 = K_2$, $t_{01} = t_{02}$. The models were compared using residual sum of squares (RSS) and Akaike Information Criterion (AIC). Statistical significance was determined at a threshold of $p < 0.05$.

GROWTH STRATEGY

In addition to age in days, OTOLab also recorded every DGI width, related to the individual's growth per day. On the SS ×1000, the first to the 30th DGI widths were recorded from the first feeding check (FFC), and corresponded to the larval life of the individuals sampled. The growth corresponding to the recruit and juvenile phases was inferred from the readings in the ×200 and ×400 sections along the posterior growth axis, from the end of the larval zone to the edge of the otolith. To standardise the readings, sagittal readings ×1000 were considered for the area corresponding to larval growth in all FS measurements.

A daily growth pattern was then estimated using the mean DGI width obtained from all the readings taken from the otolith samples. The mean DGI width (equating them to the birth date, despite birth dates being different) was used to observe the growth strategy of the population and to establish the life stages where growth was higher and lower.

VALIDATION

First, otolith radius (OR) vs TL relationship were compared between whole otoliths and sections to validate measurements throughout posterior axis. This analysis aimed to evaluate whether the linear relationships between `TL mm` (explanatory variable) and `OR mm` (response variable) differed between two groups defined by the factor `magn` (`FSx200` and `SSx20`). A linear regression model was fit for each group separately using the formula `OR mm ~ TL mm`. A combined model including an interaction term was fit to assess differences between the groups: OR mm = $\beta_0 + \beta_1$ * TL mm + β_2 * magn + β_3 * (TL mm * magn). The interaction term evaluated whether the slopes (i.e., the relationships between `TL mm` and `OR mm`) differed between the groups. An ANOVA was also performed to compare the combined model with interaction (`OR mm ~ TL mm * magn`) against a simpler model without interaction (`OR mm ~ TL mm + magn`). Statistical significance was assessed at the 5% level (p-value < 0.05).

From growth strategy results we can observe how DGI widths patterns change along the individuals age (increment number form birth), along the otolith size (OR) and along total size (TL). These results were then contrasted with microstructure annual ring measurements and first maturity references for this species, zone and year. Furthermore, the hatching (birth) date was estimated by subtracting the estimated total age (in days) from the sampling date (catch date). To verify whether the anchovy cohorts matched the spawning peaks of anchovy (July/August), we analysed the estimated birth date distribution.

RESULTS

Of the initial 53 right frontal sections [FS]), a total of 40 FS (63%) were finally readable (Table 1). Overall, the central zone of the SS (CZ_S, x1000) enabled visualisation of the DGI during the larval and post-larval stages of anchovy in 31 SS (58%) (Table 1). DGI were counted and measured from the first feeding check (FFC, Figure 2c), located at a mean distance of 11.4 µ (range 5.4–18.25 µ, SD 2.86) from the otolith nucleus along the posterior axis. The number of DGI plotted against the radius readings provided a linear relationship (R^2 = 0.65), which was subsequently used to calculate the number of days corresponding to the unreadable in FS (Figure 3).

As the initial DGI counting on FS did not include larval life increments, they could not be properly assumed as corresponding to ages. Total ages were finally obtained for the FS, at two different magnifications, once the counted larval life increments were added to the readings.

The VBGM was successfully fitted to both groups (Figure 4). The parameter estimates for FSx200 were L_∞ = 18.34 mm (p < 0.001), K = 2.97 (p = 0.1255), and t_0 = 0.22 (p = 0.0567). For FSx400, the estimates were L_∞ = 17.30 mm (p < 0.001), K = 3.83 (p = 0.0414), and t_0 = 0.23 (p = 0.0037) (Table 2a).

The likelihood ratio test showed no statistically significant differences between the growth parameters of FSx200 and FSx400: (Table 2b). Model comparisons using AIC indicated that the most parsimonious model was the null hypothesis ($L_\infty 1 = L_\infty 2$, $K_1 = K_2$, $t_{01} = t_{02}$), with an AIC of 362.9. Residual diagnostics showed no significant patterns, confirming the adequacy of the fitted models. These results suggest that the growth parameters do not differ significantly between FSx200 and FSx400 under the conditions studied.

Larval life and growth strategy were analysed using 31 SS at ×1000. In this study, the results showed that the mean FFC was located at 11.4 µm (range 5.4–18.25, SD 2.86) from the nucleus, with a mean observed radius of 118.19 µm (range 30.90–226.59, SD 46.9). The observed mean larval lifespan was 27 days. The daily growth pattern estimated by the mean DGI width from all the readings performed throughout the CZ_S showed that mean DGI widths increased progressively from 2.04 to 6.12 µm (mean [4.13 ± 1.26] µm) at the end of the first month of life. Larval life DGI widths are represented for the first 30 days in Figure 5 a (red circles correspond to SS x1000 readings). In this area DGI progressively increased, had a regular appearance and almost a complete absence of subdaily microincrements.

Juvenile and adult growth strategies were analysed from the results of each method (FS ×200, FS ×400) (Figure 5). The range of DGI widths was ample (Table 3), from 0.82 to 29.32 µm, when both methods were considered together, along with increments from the 31st, but excluding those corresponding to the larval phase (1st–30th). Recruits and immature juveniles < 6 cm TL (ranging approximately from 50 to200 days) were characterised by the presence of wider microincrements and higher interindividual variability (Figure 5c). In this area, the DGI pattern was mostly regular, though it occasionally reached more than 25 µm-width. Thereafter, from 200 days, mean DGI width progressively decreased in the juvenile phase and remained steady throughout the adult phase.

In conclusion, the similarity between the results in the FS in both magnifications under the microscope, both in the VBGM models (Figure 4, Table 2) and in the growth strategies (Figure 5a), make us opt for the FSx200 option as the most practical for assigning ages in anchovy. Therefore, it is the one we will use for the validation objective.

Model coefficients for otolith radius (OR) vs TL linear models (Figure 6) showed not statistical differences between FSx200 and whole otoliths (SSx20): i) The interaction term (`TL mm:magn`) in the combined model was not statistically significant (p = 0.769), indicating no evidence that the slopes differ between the groups, ii) similarly, the group-level coefficient (`magn`) was also not significant (p = 0.657), suggesting no significant difference in intercepts. The ANOVA comparing the models with and without interaction yielded a p-value of 0.769, confirming that adding the interaction term did not improve the model significantly. Therefore, the simpler model without interaction (`OR mm ~ TL mm + magn`) was adequate to explain the relationship. The analysis concluded that the relationship between `TL mm` and `OR mm` does not differ significantly between the groups `FSx200` and `SSx20`. Both slopes and intercepts were statistically equivalent, and the simpler model without interaction provided an adequate fit.

From a total of 793 whole otoliths (72–171 mm TL) analysed, the first winter annulus (R1) was identified and measured in 194 otoliths (107–171 mm TL). The R1 mean distance from the otolith nucleus along the posterior growth axis was 1.43 mm (range 1.01–1.80 mm, SD 0.15) (Figure 7).

The results from the relationship between otolith radius OR and anchovy TL (Figure 6), along with the growth model proposed in this study for the anchovy in the Alboran Sea (Figure 4), allowed us to correlate R1 formation with age (Figure 5a), OR (Figure 5b) and TL (Figure 5c). Thus, the mean distance to the first hyaline R1, measured through the otolith posterior axis, was 1.43 mm, corresponding to 12.1 cm TL (Figure 6), and an age of 210 days (7 months).

Analysis of birth date distribution from FS ×200 readings showed that the individuals were born between March and

December 2013, and peaked in July (30%), followed by June and May (17.5% for both months). Percentages were below 7.5% for the rest of the year (Table 4).

DISCUSSION

Obtaining age data from the calcified structures of fish to regulate their stocks entails considerable investment in material and human resources. New methods and tools are then required to facilitate this task, in the search for more reproducibility and, if possible, to improve measurement precision. Despite the technological advances and enormous possibilities of digital tools and artificial intelligence, the basis of scientific progress in this field still depends on the quality of the samples, the right tools and the biological knowledge of growth experts. Once the best methods have been established, it will be easier to confirm the standards of each species and to automate processes. State-of-the-art automating processes have already been established for analysing otolith macrostructure in several species (Fablet and Le Josse, 2005; Kemp and Doherty, 2022), though not yet in microstructure.

This work is, primarily, a methodological study, aimed at offering new and improved tools for determining age from otoliths particularly in anchovy and extendible to other species, as has been already done in hake (Piñeiro et al., 2008; Rey et al., 2016). Secondarily, it is a validation study for the Alboran Sea anchovy. A sample of anchovy otoliths was selected to develop the method and to compare it with existing studies on this species.

Otolith microstructure, first described by Panella (1971), has been explored in numerous fish species (Campana and Neilson, 1885; Stevenson and Campana, 1992; Panfili et al., 2002), and DGI formation has been confirmed throughout all fish life periods, both in the marine environment (Aldanondo et al, 2016; Panfili et al., 2002; Piñeiro et al, 2008; Plaza and Cerna, 2015; Rey et al, 2016; Sardenne et al. 2015; Spich and Fey, 2022) and in culture (Alemany and Álvarez, 1994; Morales-Nin et al., 2005; Soares et al., 2021; Tonheim et al., 2020). These accurate microstructures still offer numerous possibilities, since they will lead to a deeper understanding of the interaction between the exploited species and the environment, and to the possibility of quantifying their impact (Sponaugle, 2010).

Previous studies on anchovy otolith microstructure (Aldanondo et al., 2011; Cermeño et al., 2003; Cermeño et al., 2008; Cerna and Plaza, 2016) were carried out along the posterior growth axis of the sagittal section (SS) of otoliths. To compare our results, we counted along the posterior axis when changing to another plane, which was only possible with frontal sections (FS), since the transversal section (TS) commonly used in other species has no posterior growth axis (Figure 1a).

Following the growth studies outlined above, the use of SS microstructure in anchovy has yet to develop any enhanced method for routinely assigning ages, mostly due to the complexity of the process (as detailed below). Moreover, several authors agree that SS are more difficult to use when ageing other species, such as hakes (Piñeiro et al., 2008; Rey et al., 2016). Otoliths are three-dimensional structures, with a slight sagittal (concave/convex) curve. Consequently, the otolith edge, or centre, is easily lost when it is polished along the SS, because of varying heights and thicknesses. Although we occasionally manage to obtain a section from the centre to the edge, it is difficult to work along the same growth axis in different samples. The readings in different samples are therefore not strictly comparable. However, the SS is recommended for analysing the microstructure of particular locations in the otolith, such as the nucleus (recording the larval phase events) or the edge (recording recent growth), where increments

are usually narrower and thus frequently require higher magnification (Aldanondo et al., 2008; 2016; Cermeño et al., 2003; García et al., 2003; Rey et al., 2016). We have here obtained comparable results when comparing OR measurements and TL, both in whole otoliths (SS x20) and sections (FS x200) (Figure 6).

Other possible planes that contain the centre of the otolith are TS and FS (Wright et al., 2002). From these we can certainly obtain a section with a uniform width, thus reducing the risk of losing the centre or edge during the polishing process. It thus becomes easier to obtain the same growth axis in all the sampled otoliths, and consequently to compare readings. However, the central region is rarely clear enough to analyse the microincrements. To solve this problem, we combined larval life readings in SS ×1000 with juvenile life readings obtained in different ways, following Piñeiro et al. (2008) and Rey et al. (2016).

Furthermore, the entire process is time--consuming, and SS often present overpolished areas, both in the nucleus and in areas near the edges of the otolith, thereby hindering age determination. When the number of discarded otoliths was compared, SS surpassed the rejected FS (Table 1). Otolith fractures were much more common in the SS during handling, which made obtaining readable sections more complicated.

In the present study, two magnifications (FS at ×200 and FS at ×400) were tested to find alternative ways of analysing anchovy otoliths. The approach to age-reading using the FS proved to be successful with anchovy otoliths. In fact, growth models (Figure 4, Table 2) adjusted for each method showed that readings estimated by FSx200 and FSx400 fitted similarly. These results suggest that the growth parameters do not differ significantly between FSx200 and FSx400 under the conditions studied (Table 2b). The K-parameter ranged from 2.97 (TS ×200) to 3.83 (TS ×400), and both models showed a fast growth strategy: most of the sampled individuals were less than one-year-old.

A lower magnification (×200) makes it easier for the reader to scroll down the image and thus have a better overview of the growth pattern. Moreover, the lower magnification results in fewer images needing to be taken and overlapped, thereby reducing handling time and facilitating the entire process. Therefore, the results of this study show that counting along the FS at ×200 magnification is the best method for regularly ageing juveniles and adult anchovy. FS were easier to handle, and the final polishing made it possible to distinguish the DGI more clearly, thereby considerably reducing the risk of overpolishing some areas. Also, in many cases, FS revealed clearly visible DGI in their central area. However, in this study, SS ×1000 merely served to estimate growth during the larval phase, which was done by counting the DGI in the central zone of the SS (CZ_S). Also, the birth dates calculated by FSx200 (Table 4), fitted the spawning dates obtained by other authors (July) (Giráldez and Abad, 1995; Palomera, 1992).

Macrostructural data place the ring, typified by experts as the first winter ring, at a mean distance of 1.43 mm from the otolith nucleus (Figure 7), corresponding to individuals of 12.1 cm TL (Figure 6). This result coincides with that obtained by Ventero et al. (2017) for anchovy from the same area (West Mediterranean Alboran Sea GSA01) and year (2014). Based on the accepted VBGM based on FS at ×200 (Figure 4, Table2), a 12-cm individual is seven months old when it forms the first winter ring, and in the first year North Alboran anchovy reach 16.52 cm. Given that birth was in July (Giráldez and Abad, 1995; Palomera, 1992), in reality it corresponds to a ring formed in winter (December to February), which does not indicate a complete year of life, but coincides with sexual maturation (Girál-

dez and Abad, 1995; Basilone et al., 2004; Basilone et al., 2006; Palomera et al., 2003). Thus, as already indicated in other species, the main hyaline ring in the otoliths marks a biological and not an environmental event, such as winter (Rey et al., 2016), coinciding with a decreasing DGI widths period (Figure5). This biological event can be the onset of sexual maturity, when part of the energy directed to growth goes to gonad formation (Rey et al., 2016). Particulaly, Northern Alboran Sea anchovy first maturation (L_{50}) was calculated at 9.7 cm in 2014 and at 10.3 cm for the period between 2004 y 2014 (Giraldez et al., 2014). All these results have been summarized and shown as a whole in Figure 8, in order to improve the understanding of this work.

In conclusion, this study has satisfactorily achieved its initial goal of improving the methodological technique of routinely ageing anchovy by suggesting FS analysis at ×200 magnification as an appropriate alternative method. Secondarily, there is also evidence of the biological influence on the first winter ring formation, which also reinforces the validity of the proposed method. Biological events may obviously be combined with environmental or seasonal events, which may add to their effects on the formation of hyaline rings in the otolith (Aldanondo et al., 2016). These issues should be further investigated.

Globally, otolith microstructure analysis is currently a promising alternative option for regularly ageing juveniles and adult fish (ICES, 2019). We would also highlight, based in our practise, that technical experience in the otolith handling and polishing process is of paramount importance for obtaining high quality otolith slices that are readable. Efforts should therefore be made in this aspect, to improve growth studies in future. Our results suggest that this methodology, combining SSx1000 and FSx200 DGI readings, is feasible and easily applicable to other anchovy stocks and probably to other short life species. However, it is the task of the experts to use these methods to obtain their own results, and to take advantage of these techniques as an indirect method of validating both annual winter and false rings (checks). Furthermore, these methods may help with other current difficulties in anchovy age readings (ICES, 2016). Each stock has its life history traits and evolution. Age and growth data are of great interest for an understanding of the dynamics of the stocks and their interactions with the environment.

REFERENCES

Aldanondo N, Cotano U, Etxebeste E, Irigoien X, Álvarez P, Martínez de Murguía A and DL Herrero. 2008. Validation of daily increments deposition in the otoliths of European anchovy under different temperature conditions. *Fisheries Research,* 93: 257–264.

Aldanondo N, Cotano U, Tiepolo M, Boyra G and X Irigoien. 2010. Growth and movement patterns of early juvenile European anchovy (*Engraulis encrasicolus* L.) in the Bay of Biscay based on otolith microstructure and chemistry. *Fisheries Oceanography,* 19: 196–208.

Aldanondo N, Cotano U and E Etxebeste. 2011. Growth of young-of-the-year European anchovy (*Engraulis encrasicolus*, L.) in the Bay of Biscay. *Scientia Marina,* 75: 227–235.

Aldanondo N, Cotano U, Álvarez P and A Uriarte. 2016. Validation of the first annual increment deposition in the otoliths of European anchovy in the Bay of Biscay based on otolith microstructure analysis. *Marine and Freshwater Research*, 67: 943–950.

Alemany F, and F Álvarez. 1994. Formation of initial daily increments in sagittal otoliths of reared and wild Sardina pilchardus yolk-sac larvae. *Marine Biology*, 121: 35–39.

Basilone G, Patti B, Bonanno A, Cuttitta A, Vergara AR, García A, Mazzola S and G Buscaino. 2004. Reproductive aspects of the European anchovy (*Engraulis encrasicolus*): six years of observations in the Strait of Sicily. *MedSudMed Technical Documents* No. 5: 67-78.

Basilone G, Guisande C, Patti B, Mazzola S, Cuttitta A, Bonanno A, Vergara AR and I Maneiro. 2006. Effect of habitat conditions on reproduction of the European anchovy (*Engraulis encrasicolus*) in the Strait of Sicily. *Fisheries Oceanography*, 15 (4): 271-280.

Basilone G, Barra M, Ferreri R, Mangano S, Pulizzi M, Giacalone G, Fontana I, Aronica S, Gargano A, Rumolo P, Genovese S and A Bonanno. 2020. First annulus formation in the European anchovy; a two-stage approach for robust validation. *OPEN Nature Research Scientific Report* 10: 1079. https://doi.org/10.1038/s41598-020-58174-5

Beamish RJ and GA Farlane. 1983. Validation of Age Determination Estimates: The Forgotten Requirement. *NOAA Technical Report,* NMFS 8198329-33.

Campana SE. 2001. Accuracy, precision and quality control in age determination, including a review of the use and abuse of age validation methods. *Journal of fish biology*, 59: 197–242.

Campana SE and JD Neilson. 1985. Microstructure of fish otoliths. *Canadian Journal of Fisheries and Aquatic Sciences*, 42: 1014–1032.

Campana SE and SR Thorrold, 2001. Otoliths, increments, and elements: keys to a comprehensive understanding of fish populations? *Canadian Journal of Fisheries and Aquatic Sciences*, 58: 30–38.

Campana, SE, 2005. Otolith science entering the 21st century. *Marine and Freshwater Research*, 56: 485–495

Cermeño P, Uriarte A, De Murguía AM and B Morales-Nin. 2003. Validation of daily increment formation in otoliths of juvenile and adult European anchovy. *Journal of Fish Biology*, 62: 679–691.

Cermeño P, Uriarte A, Morales-Nin B, Cotano U and P Álvarez, 2008. Setting up interpretation criteria for ageing juvenile European anchovy otoliths. *Scientia Marina,* 72: 733–742.

Cerna F and G Plaza, 2016. Daily growth patterns of juveniles and adults of the Peruvian anchovy (*Engraulis ringens*) in northern Chile. *Marine and Freshwater Research*, 67: 899–912

Dortel E, Massiot-Granier F, Rivot E, Million J, Hallier JP, Morize E, Munaron JM, Bousquet N and E Chassot. 2013. Accounting for Age Uncertainty in Growth Modeling, the Case Study of Yellowfin Tuna (*Thunnus albacares*) of the Indian Ocean. *PLOS ONE*, https://doi.org/10.1371/journal.pone.0060886

Fablet R and N Le Josse, 2005. Automated fish age estimation from otolith images using statistical learning. *Fisheries Research*, 72(2-3): 279-290.

García A, Cortés D, Ramírez T, Giráldez A and A Carpena, 2003. Contribution of larval growth rate vairability to the recruitment of the Bay of Málaga anchovy (SW Mediterranean) during 2000-2001 spawning seasons. *Scientia Marina,* 67: 477–490.

Giráldez A and R Abad. 1995. Aspects on the reproductive biology of the western Mediterranean anchovy from coast of Malaga. *Scientia Marina,* 59: 15–23.

Giráldez A. 2012. Estudio de la variabilidad temporal de los parámetros reproductivos del boquerón (Engraulis encrasicolus l.) en el mar de Alborán. Instituto Español de Oceanografía. http://hdl.handle.net/10508/507

Giraldez A, Torres P, Iglesias M, González M, Díaz N, Meléndez and A Ventero. 2015. Stock Assessment Form. Anchovy in GSA01 (Northern Alboran Sea). CGPM, FAO. 19 pp.

Hernández C, Villamor B, Barrado J, et al. 2013. Age determination in European anchovy (Engraulis *encrasicolus* L.) otoliths in the Bay of Biscay (NE Atlantic). WD to the Workshop on Micro increment daily growth in European Anchovy and Sardine (WKMIAS). ICES 21 - 25 October 2013 Mazara del Vallo, Italy.

Hilborn R and CJ Walters. 1992. Quantitative Fisheries Stock Assessment: Choice, Dynamics and Uncertainty. Chapman and Hall, New York. 570 pp.

Hunter E, Laptikhovsky VV and PR Hollyman. 2018. Innovative use of sclerochronology in marine resource management. *Marine Ecology Progress Series,* 598: 155–158. https://doi.org/10.3354/meps12664

ICES, 2009. Report of the Workshop on Age reading of European anchovy (WKARA). ICES CM 2009/ACOM:43.

ICES, 2013. Report of the Workshop on Micro increment daily growth in European Anchovy and Sardine (WKMIAS). ICES CM 2013/ACOM: 5

ICES, 2016. Report of the Workshop on Age estimation of European anchovy (*Engraulis encrasicolus*) (WKARA2). ICES CM 2016/SSGIEOM: 17

ICES, 2019. Report of the Workshop on Age validation studies of small pelagic species (WKVALPEL). ICES Scientific Reports. 2:15. 76 pp. http://doi.org/10.17895/ices.pub.5966

ICES, 2023. Workshop 3 on age estimation of European anchovy (*Engraulis encrasicolus*) (WKARA3; outputs from 2012 meeting). ICES Scientific Reports. 5:46. 59 pp. http://doi.org/10.17895/ices.pub.22725719

Kemp CE and SK Doherty, 2022. Determining salmon provenance with automated otolith reading. *Fisheries Research*, 250: 106295. doi: https://doi.org/10.1101/2021.10.14.464436

Kimura DK 1980. Likelihood methods for the von Bertalanffy growth curve. U. S. *Fisheries. Bulletin*, 77(4): 765-776.

Morales-Nin B, Bjelland R and E Moksness. 2005. Otolith microstructure of a hatchery reared European hake (*Merluccius merluccius*). *Fisheries Research*, 74: 300–305.

Nava E, Villar EI, Clemente MC, Rey J, García A, Fernández-Peralta L, Piñeiro CG and P Otero. 2018. Digital Imaging Tool to Enhance Otolith Microstructure for Estimating Age in Days in Juvenile and Adult Fish. *IEEE Journal of Oceanic Engineering*, 43(1):48–55.

Nelson GA. 2023. _fishmethods: Fishery Science Methods and Models_. R package version 1.12-1, https://CRAN.R-project.org/package=fishmethods.

Palomera I, Morales-Nin B and J Lleonart, 1988. Larval growth of anchovy, *Engraulis encrasicolus*, in the Western Mediterranean Sea. *Marine Biology,* 99: 283–291.

Palomera I. 1992. Spawning of anchovy *Engraulis encrasicolus* in the Northwestern Mediterranean relative to hydrographic features in the region. *Marine Ecology Progress Series*, 79: 215-223.

Palomera I, Tejeiro B, and X Alemany. 2003. Size at first maturity of the NW Mediterranean anchovy. Document Presented to the GFCM e SAC Subcommittee on Stock Assessment Working Group on Small Pelagic Species, Tanger, Morocco, March 2003. 6 pp

Palomera I, Olivar MP, Salat J , Sabatés A, Coll M, García A and B Morales-Nin, 2007. Small pelagic fish in the NW Mediterranean Sea: An ecological review. *Progress in Oceanography*, 74: 377–396.

Panella G, 1971. Fish otoliths: daily growth layers and periodical patterns. *Science* 173: 1124–1127.

Panfili J, de Pontual H, Troadec JP and PJ Wright (Eds.) 2002. Manual of Fish Sclerochronology. Ifremer-IRD, Brest, France. 463 pp. https://doi.org/10.1111/j.0022-1112.2005.0751d.x

Piñeiro C, Rey J, de Pontual H and A García, 2008. Growth of Northwest Iberian juvenile hake estimated by combining sagittal and transversal otolith microstructure analyses. Fisheries *Research,* 93: 173–178.

Plaza G and F Cerna, 2015. Validation of daily microincrement deposition in otoliths of juvenile and adult Peruvian anchovy *Engraulis ringens*. *Journal of Fish Biology,* 86: 203–216.

Rey J, Fernández-Peralta L, García A, Nava E, Clemente MC, Otero P, Villar EI and CG Piñeiro, 2016. Otolith microstructure analysis reveals differentiated growth histories in sympatric black hakes (*Merluccius polli* and *Merluccius senegalensis*). *Fisheries Research*, 179: 280–290.

Sardenne F, Dortel E, Le Croizier G, Million J, Labonne M, Leroy B, Bodin N and E Chassot. 2015. Determining the age of tropical tunas in the Indian Ocean from otolith microstructures. *Fisheries Research*, 163: 44-57.

Schneider C, Rasband W and K Eliceiri. 2012. NIH Image to ImageJ: 25 years of image analysis. *Natural Methods*, 9: 671–67. https://doi.org/10.1038/nmeth.2089

Soares C, Ferreira S, Ré P, Teodósio MA, Santos AM, Batista H, Baylina N and S Garrido. 2021. Effect of Temperature on the Daily Increment Deposition in the Otoliths of European Sardine *Sardina pilchardus* (Walbaum,1792) Larvae. *Oceans* 2021, 2; 723–737.

Spich, K and Fey DP. 2022. Using otolith microstructure analysis in studies on the ecology of the early life stages of cod, *Gadus morhua* L.: A review. *Fisheries Research,* 250: 106265.

Sponaugle S. 2010. Otolith microstructure reveals ecological and oceanographic processes important to ecosystem-based management. *Environmental Biology of Fishes,* 89(3): 221–238.

Stevenson DK and SE Campana. 1992. Otolith Microstructure Examination and Analysis. *Canadian Special Publication of Fisheries and Aquatic Sciences,* 117: 126 pp.

Tonheim S, Slotte A, Andersson L, Folkvord A and F Berg. 2020. Comparison of Otolith Microstructure of Herring Larvae and Sibling Adults Reared Under Identical Early Life Conditions. *Frontiers on Marine Science* (7). https://doi.org/10.3389/fmars.2020.00529

Torres P, Ramírez JG, Garriga M, Silvestre M, Iglesias M, González M and A Ventero. 2022. Anchovy (*Engraulis encrasicolus*) Stock Assessment in the GFCM GSA01, Northern Alborán Sea, RY2021. GFCM. *Working Group on stock assessment of Small Pelagic Species*.

Uriarte A, Prouzet P and B Villamor. 1996. Bay of Biscay and Ibero Atlantic anchovy populations and their fisheries. *Scientia Marina,* 60; 237–255.

Uriarte A, Rico I, Villamor B, Duhamel E, Dueñas C, Aldanondo N and U Cotano. 2016. Validation of age determination using otoliths of the European anchovy (*Engraulis encrasicolus* L.) in the Bay of Biscay. *Marine and Freshwater Research*, 67(7); 951–966. https://doi.org/10.1071/MF15092

Ventero A, Iglesias M and B Villamor. 2017. Anchovy (*Engraulis encrasicolus*) otoliths reveal growth differences between two areas of the Spanish Mediterranean Sea. *Scientia Marina*, 81(3): 327–337.

Villamor B, Dueñas-Liaño C, Hernández C, Antolinez A and MR Navarro. 2019. Criterios de Interpretación de la Edad en los Otolitos de la Anchoa europea (*Engraulis encrausicolus*) del Golfo de Vizcaya. Documento Interno del IEO, Proyecto BIOPEL, Abril 2019. Repositorio del IEO.

Whitehead PJP, Nelson GJ and T Wongratana. 1988. Clupeoid Fishes of the World (Suborder Clupeoidei): An Annotated and illustrated catalogue of the herrings, sardines, pilchards, sprats, shads, anchovies and wolf-herrings.Part 2. Engraulidae. FAO Fish. Synop. (125) Vol 7. Pt. 2: 305–579.

Wright PJ, Panfili J, Morales-Nin B and AJ Geffen. 2002. Otoliths, In: Panfili, J., de Pontual, H., Troadec, J-P., and Wright, P. J. (Eds.) Manual of Fish Sclerochronology. Ifremer-IRD Co-edition, Brest, France 31–57.

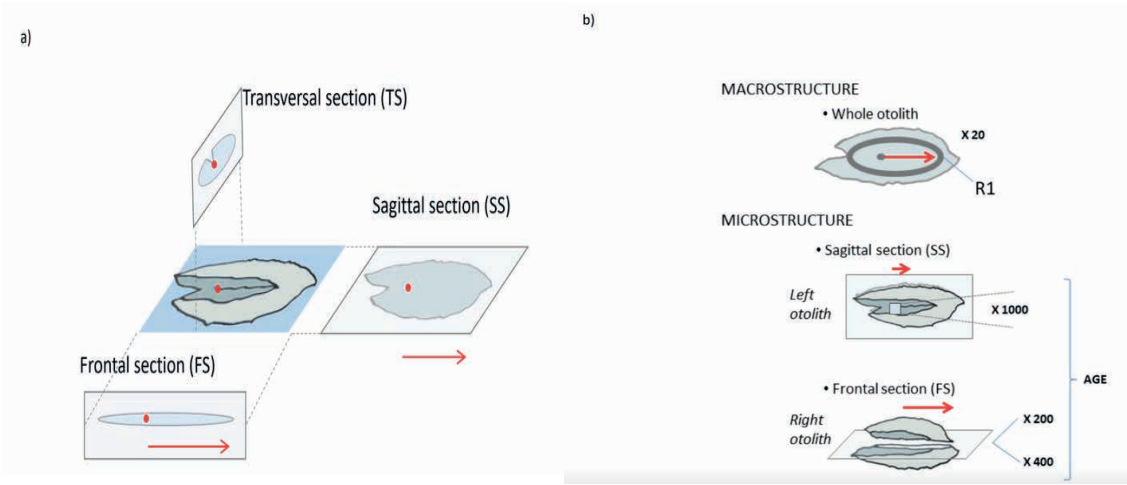

Figure 1. a) Otolith sections, with highlighting of otolith centre (red dots) and posterior growth axis (red arrows). b) Polishing process scheme: left otoliths were polished using the sagittal section (SS) and right otoliths using the frontal section (FS). FS were then read at ×200/×400 magnifications along the posterior axis (red arrow). Nucleus primary growth increments were visible in detail at ×1000 magnification in the SS.

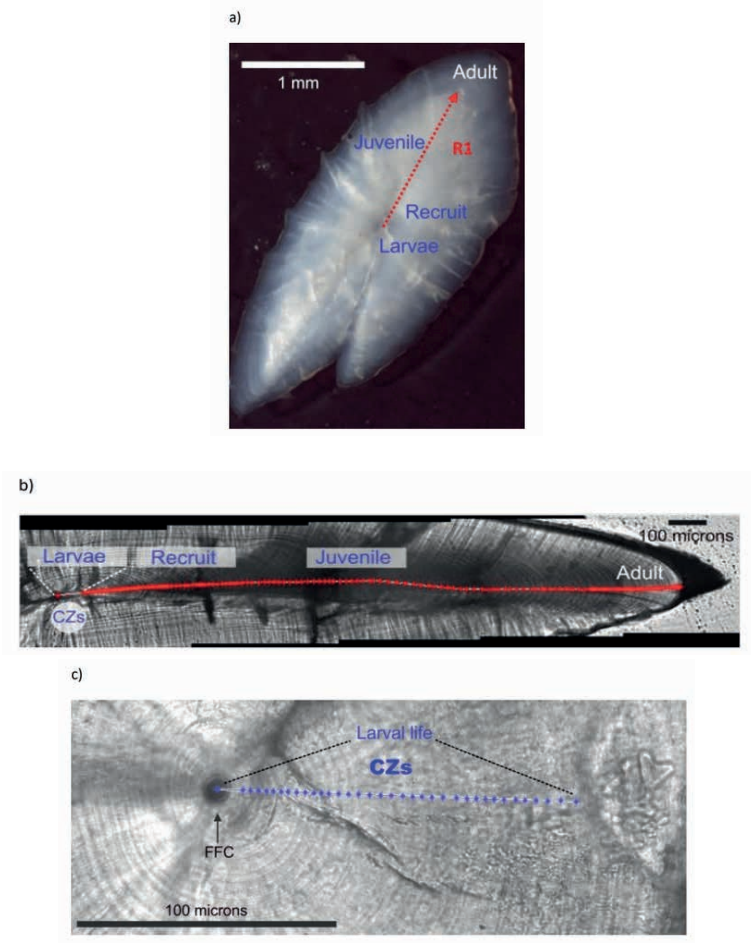

Figure 2. a) whole otolith (×20) indicating the first winter ring (R1) along the posterior axis, b) otolith frontal section (FS) (×200) and c) nucleus in otolith SS (×1000), showing the digital growth increments (DGI) readings

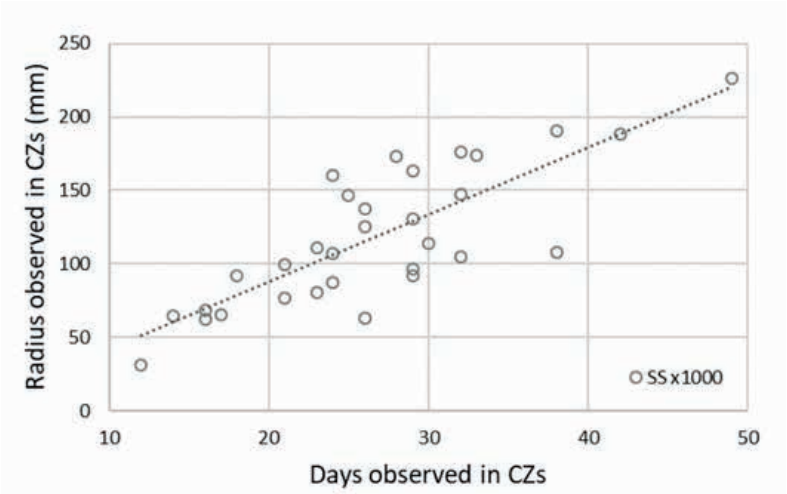

Figure 3. Larval life model that relates the number of daily growth increments observed in the central zone of the sagitta (CZ_s) and the radius of CZ_s ($R^2 = 0.65$). Model equation: larval age (days) at the central zone = radius observed/4.5708 + 3.5979

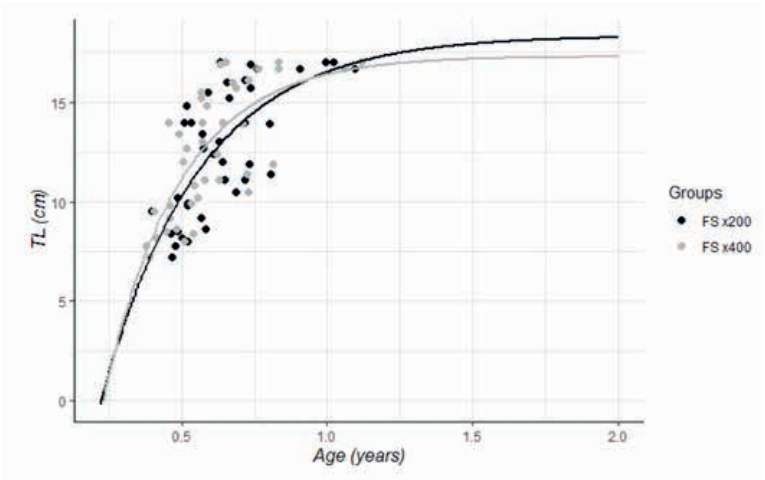

Figure 4. Typical Von Bertalanffy Growth Model final models: Frontal section (FS) ×200/×400; TL = Total length (cm).

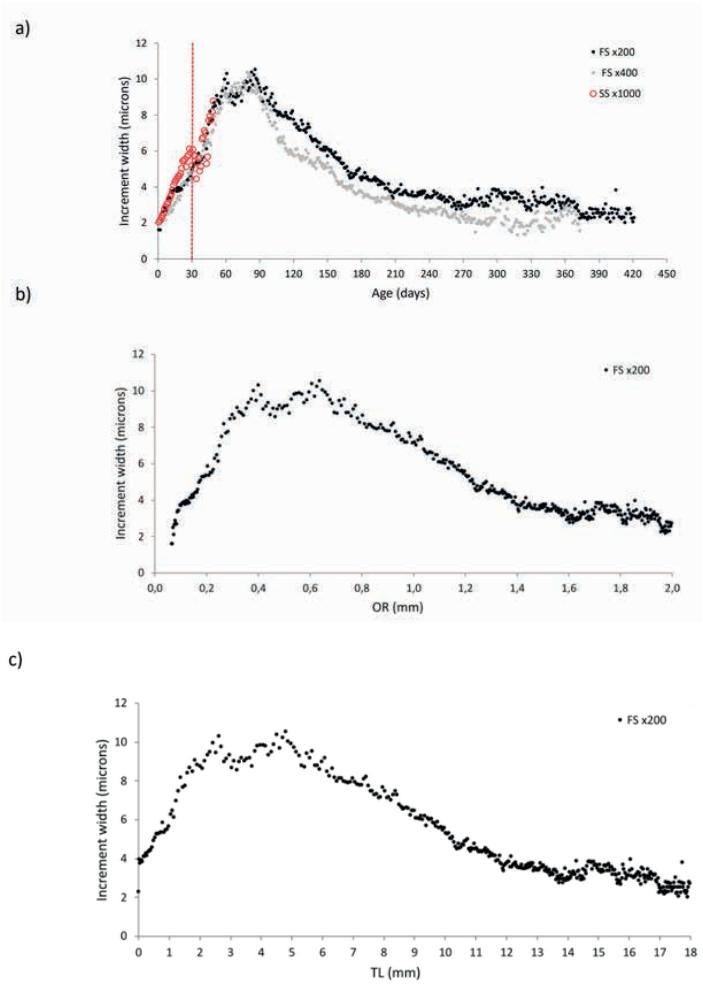

Figure 5. a) Average increment widths by age from the otoliths using both magnifications of this study: Frontal section (FS). Red circles indicate results from SS ×1000, corresponding to larval growth. b) Average increment widths by OR. c) Average increment widths by TL.

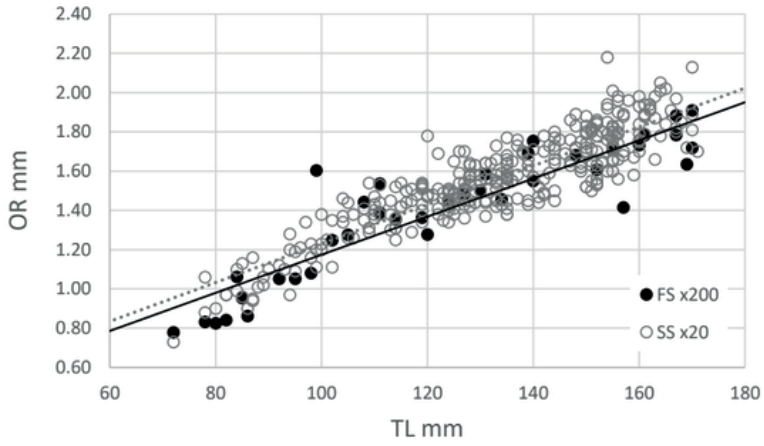

Figure 6. Otolith radius (OR) on posterior axis vs total length (TL) in whole otoliths (SS x20) and FS x200.

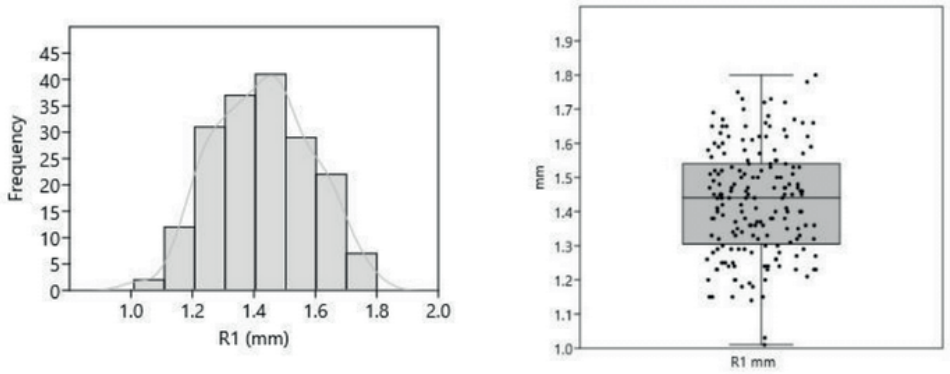

Figure 7. R1 measures along the posterior axis (SS x20): a) frequency distribution and b) box plot.

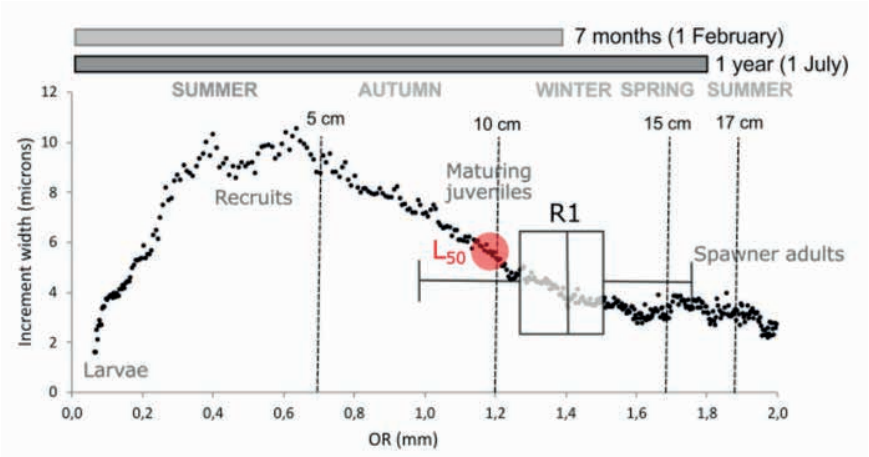

Figure 8. Theoretical scenario among DGI widths and OR (FS x200), R1 measures, TL, age and sexual first maturity (L_{50}, from Giráldez et al., 2015).

a)

OTOLITH microstructure	Total polished		Left otoliths (SS) used for larval life (×1000)	Right otoliths (FS) used for age determination
	Left otoliths	Right otoliths		
N	53	53	31	40
TL (mm)	70–170		78–170	72–170

b)

OTOLITH macrostructure	Whole otoliths used for annual age determination	Whole otoliths with 1st winter ring (R1)
N	793	194
TL (mm)	72–171	107–171

Table 1. Summary of total otoliths: a) polished and those readable for age determination in the study. N: number of otoliths; TL: total length (mm); SS (sagittal section) and FS (frontal section), and b) whole otoliths used for annual age determination and first winter ring (R1) location.

a)

Parameter	FS200	FS400
L_{inf}	18.34 ± 3.27	17.30 ± 2.06
K	2.97 ± 1.90	3.83 ± 1.81
t_0	0.22 ± 0.11	0.23 ± 0.07
TL 1 year cm	16.52	16.40
TL 2 year cm	18.25	17.28

b)

test	hypotesis	χ^2	Df	p	rss	AIC
Ho	General model	-	-	-	367.002	362.900
Ho vs H1	$L_\infty 1 = L_\infty 2$	0.09	1	0.764	367.408	360.990
Ho vs H2	$K_1 = K_2$	0.12	1	0.729	367.546	361.020
Ho vs H3	$t_{01} = t_{02}$	0.00	1	1.000	367.016	360.900
Ho vs H4	$L_\infty 1 = L_\infty 2, K_1 = K_2, t_{01} = t_{02}$	2.00	3	0.572	376.291	358.897

Table 2. a) Von Bertalanffy estimates (±SE) for both magnification results and total lengths (cm) corresponding to years 1 and 2. b) Von Bertalanffy comparison results.

Section	Magnif.	Mean TL (mm)	Range TL	SD TL	N	Mean reading days	Range reading days	SD reading days	Range DGI width (μ)	Mean DGI width (μ)	SD DGI width (μ)
Frontal	×200	125.7	72–170	31.56	40	234	145–400	56.00	1.23–29.32	6.34	3.97
	×400	125.7	72–170	31.56	40	222	138–408	60.00	0.82–27.07	5.85	3.76
Sagittal	×1000	124.3	78–170	29.69	31	26.6	12–49	8.2	0.99–12.40	4.04	1.91

Table 3. Summary statistics of data measurements from readings along the growth axis in sagittal and longitudinal sections at two different magnifications. TL, total length; SD, standard deviation; N, number of otoliths; DGI, daily growth increments. DGI results from increment 31 (juvenile and adult phases).

MONTH 2013	FS ×200		
	N	%	TL range
January			
February			
March	2	5.0	114–139
April	3	7.5	111–140
May	7	17.5	105–167
June	7	17.5	86–157
July	12	30.0	72–170
August	3	7.5	95–170
September	1	2.5	167
October	3	7.5	160–169
November	1	2.5	167
December	1	2.5	170
	40	**100**	**72–170**

Table 4. Birth dates calculated from daily rings from FS readings at ×200. Daily Growth Increments (DGI) observed at ×1000 on sagittal section (SS) samples, corresponding to larval life, are included here.